ChemComm

View Online
Dynamic Article Links

Cite this: *Chem. Commun.*, 2011, **47**, 3784–3786

www.rsc.org/chemcomm

COMMUNICATION

Localized and propagating surface plasmon co-enhanced Raman spectroscopy based on evanescent field excitation†‡

Yu Liu, Shuping Xu, Haibo Li, Xiaoguang Jian and Weiqing Xu*

Received 16th November 2010, Accepted 17th January 2011
DOI: 10.1039/c0cc04988c

The localized and propagating surface plasmon co-enhanced Raman scattering of 4-mercaptopyridine was observed based on evanescent field excitation. The most effective coupling of the localized and propagating surface plasmons resulted in a >50 times enhanced signal relative to signals obtained on vacuum-deposited silver film.

In surface enhanced Raman scattering (SERS) detection, the effective coupling of the incident light and surface plasmons (SPs) on metal substrates plays a decisive role in obtaining high SERS signals.[1] The SPs exhibit two types: propagating and localized SPs (PSPs and LSPs)[2] and both are able to excite Raman scattering.[3–5] Many studies have been made with regard to LSP excited SERS[6] while PSP excited SERS has also been widely reported.[7,8] Theoretical prediction shows that the SERS excited by PSPs is supposed to be very low.[9] In our previous work, we coupled the incident laser by a Kretschmann surface plasmon resonance (SPR) sensor to excite the SERS spectra of analytes based on the evanescent field.[5] The optimization of the incident angle effectively couples the SPs to resonate on a vacuum-deposited metal film, obtaining enhanced signals of analytes. The enhancement factor reached 10^6, which is supposed to arise from the PSPs and to a certain extent LSPs on such a substrate[5] (see ESI†).

SERS signals can be further improved by introducing metal nanoparticles to the silver film enhanced system.[10,11] In other studies, a metal film/probe/metal nanoparticle sandwich SERS substrate was constructed by adsorbing metal nanoparticles on a continuous metal film *via* the functional groups of probe molecules, and SERS signals can be enhanced in the sandwich structures. It was considered that stronger SERS on the sandwich substrates were derived from both the electromagnetic coupling of the LSPs (on metal nanoparticles) and PSPs (on the underneath continuous metal film), and the lateral plasmon coupling between metal nanoparticles. The coupling efficiency of the SPs was roughly adjusted by varying the size of particles and the excitation wavelength of the laser.[11] In this work, we optimized the maximal coupling efficiency of the PSPs and LSPs on a silver film/4-mercaptopyridine (4-Mpy)/silver nanoparticle sandwich substrate by accurately tuning the incident angle of the excitation light. Metal nanoparticles were employed to increase the LSP contribution to acquire stronger SERS signals. The incident angle-dependent SERS spectra and the corresponding SPR curves of the silver film/4-Mpy/silver nanoparticle sandwich substrate were simultaneously measured. By detailed comparison of the incident angle-dependent SERS profiles with the SPR, we found that the maximal coupling efficiency of the PSPs and LSPs appeared at the vicinity of the SPR angle. The experimental results can help us to understand the coupling mechanism of PSPs and LSPs based on evanescent field excitation.

The SPR curves and incident angle-dependent SERS spectra were simultaneously measured by an SPR-SERS microspectrometer.[5] This is composed of three main functional parts including an incident light system, an SPR detection system and a SERS detection system (Fig. 1). The incident light system is mounted on one arm of a two-arm goniometer, composing of a laser (Changchun New industries Optoelectronics Tech. Co. Ltd), two lenses (lens 1 has a numerical aperture (NA) of 0.18 and focal length of 25 mm. lens 2 has a NA of 0.15 and focal length of 10 mm), and a polarizer. The SPR detection system comprising of lens 3 and a photodiode is

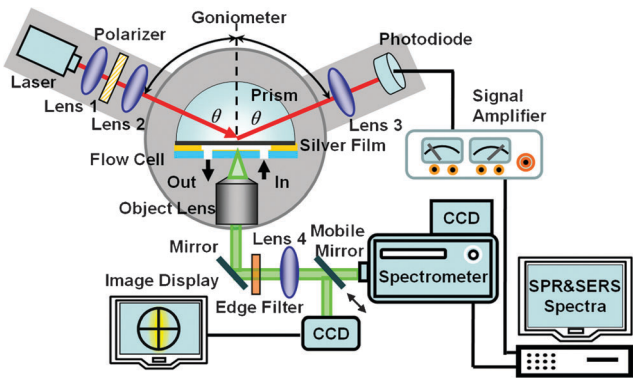

Fig. 1 Schematic diagram of the SPR-SERS microspectrometer.

State Key Laboratory of Supramolecular Structure and Materials, Jilin University, Changchun 130012, P. R. China. E-mail: xuwq@jlu.edu.cn; Fax: +8643185193421; Tel: +8643185159383

† This article is part of a ChemComm web-based themed issue on Surface Enhanced Raman Spectroscopy.

‡ Electronic supplementary information (ESI) available: LSP effect caused by the vacuum deposition of silver film, synthesis of silver nanoparticles, preparation of three different substrates, incident angle-dependent SERS spectra, calculation for the SERS enhancement factor and comparison between the evanescent field and bright field excitation. See DOI: 10.1039/c0cc04988c

fixed on the other arm of the goniometer. SPR data acquisition and precise angular rotation of the goniometer are both controlled *via* a program written by LABVIEW software (National Instruments Co.). The SERS detection system consists of three parts: an inverted microscope, a sample CCD imaging camera with a display screen, and a spectrometer (iHR320, Jobin-Yvon Co.) with a CCD (synapse, Jobin-Yvon Co.). A mobile mirror switches the light to a CCD imaging camera or a spectrometer. When the laser (532 nm) iwas focused on the surface of the silver film, part of the incident beams were reflected and then collected by the SPR detection system. At the same time, the Raman scattering of analytes was excited as well, which was collected by the SERS detection system *via* an inverted microscope with a 20× objective lens (NA = 0.35, focal length = 20.5 mm). An edge filter (λ = 532 nm, Semrock Inc.) was used to remove the Rayleigh scattering. Lens 4 (focal length = 108 mm) focused the beam to the slit of the spectrometer.

To test the coupling efficiency of the SPs we designed a variety of substrates as shown in Fig. 2. The fabrication process of the three different substrates is described in ESI‡.

Fig. 3(a) shows the SPR curves and the SERS intensity profiles obtained on the three kinds of substrates. First, we recorded the SPR curve of substrate (a) (curve A in Fig. 3(a), SPR angle = 73.78°). The spectral signals of the background (in water) were also obtained (Fig. 4S, ESI‡). Curve A-1 in Fig. 3(a) plots spectral intensities (1573 cm^{-1}) *vs.* the incident angles, showing a relatively low background. Second, the incident angle-dependent SERS spectra of 4-Mpy and the SPR curve on substrate (b) were measured *via* the SPR-SERS microspectrometer for which the resonance angle shifted from 73.78 to 73.92° (curve B in Fig. 3(a)), which indicates the adsorption of 4-Mpy on the silver film surface. The incident angle-dependent SERS signals of the 4-Mpy modified silver film are shown in Fig. 5S (ESI‡). Curve B-1 in Fig. 3(b) is the plot of SERS intensities of 4-Mpy at 1573 cm^{-1} *vs.* the incident angles. The incident angle at maximal SERS intensity is 73.00°. The SERS intensity at the resonance angles (73.00°) is about 20 times stronger than those at non-resonance angles (*e.g.* 64°), which is mainly regarded as the resonance effect from both the dominant PSPs and to a certain extent LSPs on a silver film.[5] At the vicinity of SPR angle (0.92° smaller than the resonance angle), the maximal enlarged electromagnetic field led to the highest SERS signals.[5] It should be noted that the SERS signals obtained on the substrate (b) come from the contribution of a PSP effect and the rough silver vacuum-deposited film induced LSP effect. Finally, we measured the

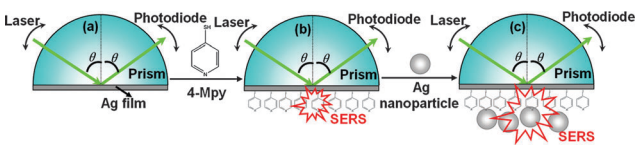

Fig. 2 (a) Schematic diagram of a Kretschmann SPR sensor. A semi-cylindrical prism was modified by a 45-nm thickness silver film. (b) Schematic diagram of SP enhanced SERS based on a vacuum-deposited silver film in which the silver film surface was further modified by 4-Mpy molecules. (c) Schematic diagram of the silver nanoparticles assisted LSP/PSP co-enhanced SERS using a silver film/4-Mpy/silver nanoparticle sandwich structure.

SPR curve (curve C in Fig. 3(a)) and the incident angle-dependent SERS spectra of 4-Mpy (Fig. 6S, ESI‡) on the sandwich substrate. The SPR angle is 73.94°, which is almost unchanged relative to the resonance angle of curve B. This may be due to the similar refractive indexes of silver nanoparticles to a silver film. We plotted the incident angle-dependent SERS signals at 1573 cm^{-1} of substrate (c) (curve C-1 in Fig. 3(a)). The maximal SERS spectrum was also obtained at an incident angle of 73.00°, which is 0.94° smaller than the SPR angle in curve C. The SERS signal at 73.00° is about 15-fold of those at non-resonance angles (*e.g.* 64°).

In substrate (c), the PSPs and LSPs induced by the rough silver film and silver nanoparticles were both involved and correlated. Apparently, the SERS signals were further enhanced after silver nanoparticles were adsorbed on the 4-Mpy modified silver film. We considered the SERS signals observed for a silver film/4-Mpy/silver nanoparticle sandwich substrate derived from the electromagnetic coupling of the SPs from silver nanoparticles and silver film. Fig. 3(b) shows two representative SERS spectra using substrates (b) and (c) when the incident angle was set to the resonance angle (73.00°). The SERS signal (at 1573 cm^{-1}) under the silver nanoparticles assisted LSP-PSP co-enhancement (upper spectrum) is more than 50 times higher than the signal obtained on the vacuum-deposited silver film (bottom spectrum). The enhancement factor (EF) for 4-Mpy adsorbed on the silver film/4-Mpy/silver nanoparticle sandwich substrate was calculated by comparing the SERS signal excited *via* an evanescent field (Fig. 7S(a), ESI‡) and the Raman signal excited *via* the total internal reflection (Fig. 7S(b), ESI‡). We compared the SERS signal at 1004 cm^{-1} on the sandwich structure excited *via* the evanescent field excitation with the Raman signal at 994 cm^{-1} excited under the total internal reflection mode. The EF is estimated to be as large as 2.0×10^7. More details for estimating the EF are provided in ESI‡.

Fig. 4(a) and (b) show the SEM images of substrates (b) and (c), respectively. It is interesting that a relatively low loading of silver nanoparticles brings about a quite strong enhancement of SERS. The electric field distribution in the system containing the prism/silver film/silver nanoparticle (by using Lumerical FDTD Solutions software, Lumerical Solutions, Inc.) is presented in Fig. 5. The electric field at the gap between the silver film and a silver nanoparticle increases by about 4000 times.

Comparing with the conventional SERS excited by a backscattering mode, the SERS signal based on the evanescent field excitation provides higher spectral quality. The SERS spectra excited and collected in an evanescent field restrain the background signals and lead to higher signal-to-noise SERS signals (see Part 6 in ESI‡), which is one of important advantages for evanescent field excited SERS.

In conclusion, we designed a silver nanoparticles assisted LSP/PSP co-enhanced spectroscopic method to detect analytes based on evanescent field excitation. The maximal SERS signal (1573 cm^{-1}) excited by the silver nanoparticles assisted LSP/PSP is about 55 times stronger than that obtained on the vacuum-deposited silver film. The maximal coupling efficiency appeared at around the resonance angles. A large SERS enhancement factor of 2.0×10^7 was obtained by the present

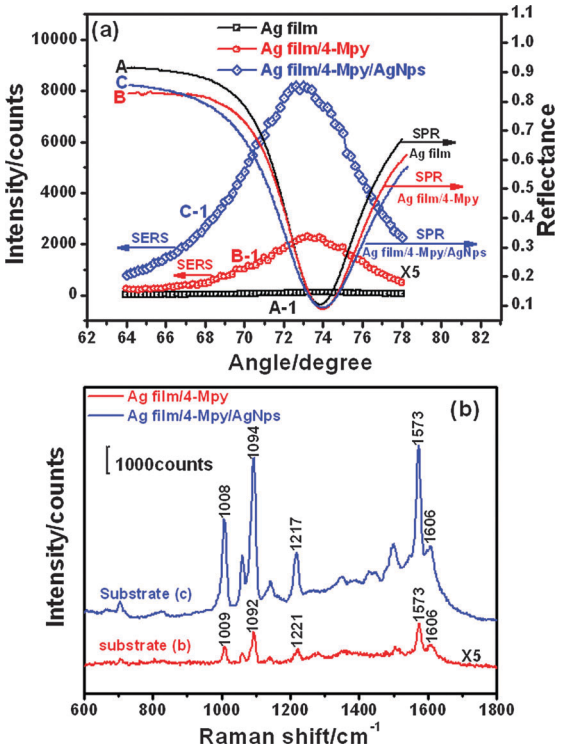

Fig. 3 (a) Curve A is the SPR curve of water. Curve A-1 is the intensity profile of the incident angle-dependent spectra, which indicates the background of water at different incident angles. Curve B is the SPR curve of substrate (b). Curve B-1 is the SERS intensity profile of the SP excited incident angle-dependent SERS of 4-Mpy on a vacuum-deposited silver film; the integration time was 3 s. Curve C is the SPR curve of substrate (c). Curve C-1 is the SERS intensity profile of the silver nanoparticles assisted LSP/PSP co-enhanced SERS of 4-Mpy on substrate (c); the integration time was 1 s. All SERS intensity profiles were obtained by plotting the SERS band intensities at 1573 cm^{-1}. The laser power was 8 mW. (b) The SERS spectra of 4-Mpy on substrate (b) and (c) at an incident angle of 73.00°.

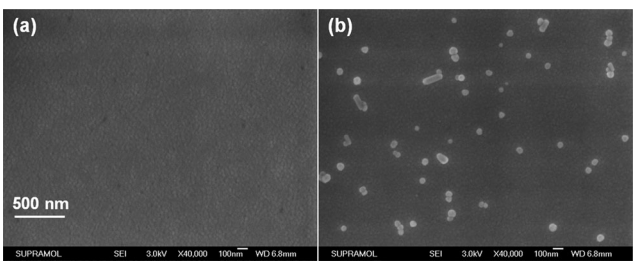

Fig. 4 (a) SEM image of a 45-nm thickness silver film. (b) SEM image of a silver film with many silver nanoparticles through 4-Mpy as a linker.

method. The effective coupling of the PSPs and LSPs provides hundreds of "hot spots" between nanoparticles and the metal film, which is hypothesized to be responsible for the additional enhancement of the SERS signals.

This work was supported by the National Natural Science Foundation of China NSFC Grant Nos. 20773045, 20903043, 20973075, 21073073 and 91027010, Research Fund for the Doctoral Program of Higher Education of China Grant No. 20090061120089.

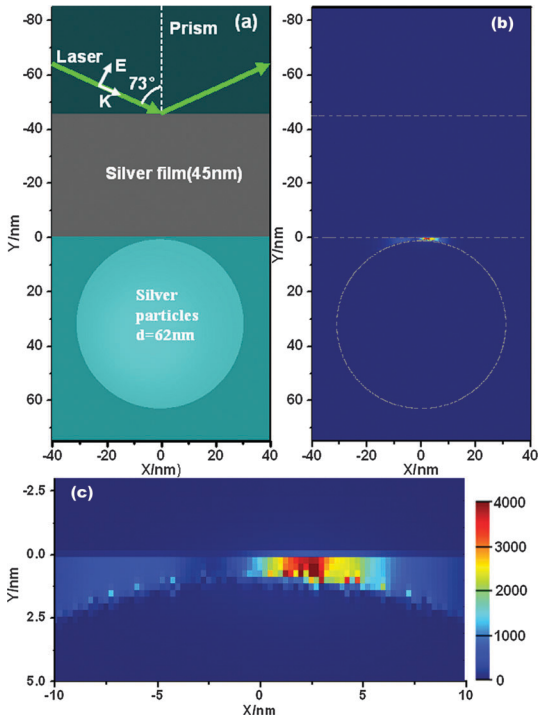

Fig. 5 (a) Schematic diagram of the prism/silver film/silver nanoparticle system used for calculation where the diameter of the silver nanoparticles is 62 nm. The dielectric surrounding around the silver nanoparticle and silver film is water. The refractive index of the prism is 1.52 at 532 nm and the thickness of the silver film is 45 nm. (b) FDTD simulation of the electric field distribution for the prism/silver film/silver nanoparticle system, with a 1-nm gap between the silver film and silver nanoparticles; *k* and *E* indicate the wavevector and electric vector of the incident light. (c) Magnification of *E* field distribution at the vicinity of the gap between a silver nanoparticle and silver film.

Notes and references

1 J. R. Lombardi and R. L. Birke, *J. Phys. Chem. C*, 2008, **112**, 5605.
2 W. L. Barnes, A. Dereux and T. W. Ebbesen, *Nature*, 2003, **424**, 824; L. S. Live, O. R. Bolduc and J. F. Masson, *Anal. Chem.*, 2010, **82**, 3780.
3 A. D. McFarland, M. A. Young, J. A. Dieringer and R. P. Van Duyne, *J. Phys. Chem. B*, 2005, **109**, 11279.
4 Y. R. Fang, H. Wei, F. Hao, P. Nordlander and H. X. Xu, *Nano Lett.*, 2009, **9**, 2049.
5 Y. Liu, S. P. Xu, B. Tang, Y. Wang, J. Zhou, X. L. Zheng, B. Zhao and W. Q. Xu, *Rev. Sci. Instrum.*, 2010, **81**, 036105.
6 X. M. Qian, X. H. Peng, D. O. Ansari, Q. Qin, Y. Goen, G. Z. Chen, D. M. Shin, L. Yang, A. N. Young, M. D. Wang and S. M. Nie, *Nat. Biotechnol.*, 2007, **26**, 83; S. M. Nie and S. R. Emory, *Science*, 1997, **275**, 1102; K. Kneipp, Y. Wang, H. Kneipp, L. T. Perelman, I. Ltzkan, R. R. Dasari and M. S. Feld, *Phys. Rev. Lett.*, 1997, **78**, 1667.
7 B. Pettinger, A. Tadjeddine and D. M. Kolb, *Chem. Phys. Lett.*, 1979, **66**, 544.
8 M. Futamata, E. Keim, A. Bruckbauer, D. Schumacher and A. Otto, *Appl. Surf. Sci.*, 1996, **100–101**, 60; M. Futamata, *Appl. Opt.*, 1997, **36**, 364; M. Futamata, *Surf. Sci.*, 1997, **386**, 89.
9 J. Giergiel, C. E. Reed, J. C. Hemminger and S. Ushioda, *J. Phys. Chem.*, 1988, **92**, 5357.
10 Q. Zhou, X. W. Li, Q. Fan, X. X. Zhang and J. W. Zheng, *Angew. Chem., Int. Ed.*, 2006, **45**, 3970; C. J. Orendorff, A. Gole, T. K. Sau and C. J. Murphy, *Anal. Chem.*, 2005, **77**, 3261.
11 J. K. Daniels and G. Chumanov, *J. Phys. Chem. B*, 2005, **109**, 17936; K. Kim and J. K. Yoon, *J. Phys. Chem. B*, 2005, **109**, 20731.

